Biophysical Chemistry 175–176 (2013) 17–27

Contents lists available at SciVerse ScienceDirect

Biophysical Chemistry

journal homepage: http://www.elsevier.com/locate/biophyschem

Simplicity within the complexity: Bilateral impact of DMSO on the functional and unfolding patterns of α-chymotrypsin

Tatyana Tretyakova [a,b], Mikhael Shushanyan [a,b], Tamar Partskhaladze [a], Maya Makharadze [b], Rudi van Eldik [c], Dimitri E. Khoshtariya [a,b,c,*]

[a] Institute for Biophysics and Bionanosciences at the Department of Physics, I. Javakhishvili Tbilisi State University, I. Chavchavadze Ave. 3, 0128 Tbilisi, Georgia
[b] Department of Biophysics, I. Beritashvili Center of Experimental Biomedicine, Gotua 14, 0160 Tbilisi, Georgia
[c] Department of Chemistry and Pharmacy, University of Erlangen-Nürnberg, Egerlandstr. 1, 91058 Erlangen, Germany

HIGHLIGHTS

- Impact of dimethyl sulfoxide on the catalytic (kinetic) pattern of α-chymotrypsin
- Impact of dimethyl sulfoxide on the unfolding/refolding pattern of α-chymotrypsin
- Interplay of stabilizing/destabilizing effects and global/local stability motifs

GRAPHICAL ABSTRACT

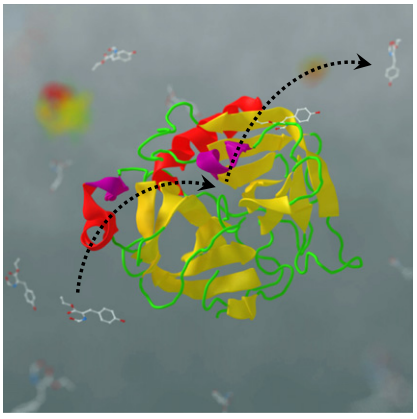

ARTICLE INFO

Article history:
Received 1 January 2013
Received in revised form 5 February 2013
Accepted 9 February 2013
Available online 26 February 2013

Keywords:
α-Chymotrypsin
Dimethyl sulfoxide
Differential scanning calorimetry
Dynamic potentiometry
Protein's local/global stability
Michaelis–Menten kinetics

ABSTRACT

New understanding of the fundamental links between protein stability, conformational flexibility and function, can be gained through synergic studies on their catalytic and folding/unfolding properties under the influence of stabilizing/destabilizing additives. We explored an impact of dimethyl sulfoxide (DMSO), the moderate effector of multilateral action, on the kinetic (functional) and thermodynamic (thermal unfolding) patterns of a hydrolytic enzyme, α-chymotrypsin (α-CT), over a wide range of additive concentrations, 0–70% (v/v). Both the calorimetric and kinetic data exhibited rich behavior pointing to the complex interplay of global/local stability (and flexibility) patterns. The complex action of DMSO is explained through the negative and positive preferential solvation motifs that prevail for the extreme opposite, native-like and unfolded states, respectively, implying essential stabilization of compact domains by enhancement of interfacial water networks and destabilization of a flexible active site by direct binding of DMSO to the unoccupied specific positions intended for elongated polypeptide substrates.

1. Introduction

Thorough understanding of protein functioning mechanisms is inseparably connected with respective issues of macromolecular stability and

* Corresponding author at: Institute for Biophysics and Bionanosciences, Department of Physics, I. Javakhishvili Tbilisi State University, 0128, Tbilisi, Georgia. Tel.: +995 322 290834 (institute), +995 322 386077 (home), +995 557 432139 (mobile); fax: +995 322 373411.
E-mail addresses: dimitri.khoshtariya@gmail.com, dimitri.khoshtariya@tsu.ge (D.E. Khoshtariya).

0301-4622/$ – see front matter © 2013 Elsevier B.V. All rights reserved.
http://dx.doi.org/10.1016/j.bpc.2013.02.006

flexibility [1–6]. The general concept of free energy hyper-surfaces, viewed as multi-functionals of essential structural variables (reaction coordinates), encompassing both, conformational and chemical (either mutually coupled, or non-coupled) transformations, may serve as a common physical basis that connects all these aspects [7–11]. The innovative motifs for such interdisciplinary studies can be introduced through the combined application of well-established and emerging experimental and computational approaches/methodologies, together with basic kinetic and thermodynamic theoretical models. In particular, new insights regarding the intrinsic links between the protein's stability, conformational flexibility and function can be gained through synergic studies of respective catalytic and/or folding/unfolding properties under the influence of stabilizing/destabilizing additives, and subsequent cross-analysis of the obtained results [12,13].

Specifically, in our earlier work [14,15], we applied the combination of dynamic potentiometric (DPM) and differential scanning calorimetric (DSC) techniques. The DPM technique, along with other kinetic methods that imply direct monitoring of protein functioning in real time, delivers information on the proteins' ability to operate under broadly variable (including extreme) experimental conditions. The proper analysis of kinetic and related activation parameters can provide fundamental insight on the relative contributions of various degrees of freedom that, according to modern theoretical notions, under different experimental conditions, may control the rate of biomolecular transformation in many different ways [1–6,12,13,16–20]. Indeed, the readily measurable kinetic/catalytic constants, along with their temperature and/or pressure coefficients (activation parameters), carry essential information about and intrinsic molecular transformations, including the role of both, intra-molecular and outer-sphere (environmental) active degrees of freedom, including conformational (dissipative) and classical/quantum chemical (inflexible) reorganizable modes [12,13,18–20] (simultaneously, related parameters, such as Michaelis constant, diffusion coefficient etc., may carry useful information about the precursor processes [12,14,15]). In contrast, the DSC technique provides information on the "global stability" and, under some assumptions, "global conversions" of globular proteins and/or their complexes, normally in a passive (nonfunctioning) situation [21–25]. The issue of "global stability", in the simplest case, can be viewed in terms of a two-state model, embracing folded and unfolded free energy "funnels" [7–11]. However, in most realistic cases, additional states including the "molten globule" or "misfolded" (aggregated) states are also involved [1,7,9,14,23–27] (see Subsection 3.4 below). Specifically, the DSC technique detects the temperature-induced unfolding (melting) process (associated with a global transition along the protein's collective conformational coordinate) as a variation of the protein's partial protein heat capacity versus temperature and, in uncomplicated cases, determines the unique "transition temperature" (temperature of thermal melting), T_m, at which concentrations of the native and thermally unfolded states are equal, and the unfolding (melting) "calorimetric enthalpy", ΔH_{cal}, that is the heat absorbed through the unfolding transformation around T_m [21–24,28].

Dimethyl sulfoxide (DMSO) is an extraordinary dipolar solvent, completely miscible with water and most organic liquids, extensively used in chemistry, biology and medicine [29–31]. The effects of DMSO are extremely diverse: specifically, it has been reported to act as a stabilizer [32,33], a denaturant [34–36], an inhibitor [37,38], an activator [39–41], and a cryoprotector/molecular chaperone [30,35,42–45]. However, its impact on α-chymotrypsin (α-CT), the model protein that is otherwise well-studied regarding both, thermodynamic (global stability) [21,22] and catalytic (enzymatic activity) [1,46] patterns, has not yet been sufficiently investigated. Some reported kinetic data indicated interesting manifestations of a dual DMSO role at distinct stages of enzymatic hydrolysis of two types of substrates by α-CT [47], vide infra. At the same time, as already mentioned above, the completed sets of results regarding the impact of urea on thermodynamic and catalytic patterns of α-CT, were reported some time ago [14,15]. Results of the earlier work encouraged us to perform new combined systematic kinetic/thermodynamic studies on the impact of DMSO, the multifaceted effector, on both, the catalytic and stability patterns of α-CT. In the present work we explored the impact of DMSO on the kinetic (functional) and thermodynamic (thermal stability) features of this archetypical enzyme for a wide range of DMSO concentrations, 0 to 70% (v/v) (0 to 10.5 M). The DSC technique was applied at pH 2.6 and 8.1, also probing the refolding aspect throughout. The DSC (i.e., thermodynamic) data were considered as a measure of the "global stability" of α-CT [1,5,12], implying the compactly folded area (domain) that serves as a supporting platform for a much more flexible active site portrayed here by way of the "local stability" [1,5,6,12,40,48–54] and probed through the Michaelis–Menten kinetic pattern (viz., the catalytic and Michaelis constant) [51–54]. The latter was examined here by the DPM technique. Both, the calorimetric and kinetic data exhibited rich behavior, pointing to the complex interplay of stabilizing/destabilizing motifs and global/local stability (and flexibility) patterns.

2. Experimental

2.1. Chemicals and solutions

Highly purified and lyophilized α-CT (EC 3.4.21.1; $M_r = 26{,}000$) was purchased from Fluka and used without further purification. The specific synthetic substrate, N-acetyl-L-tyrosine ethyl ester (ATEE) was purchased from Acros Organics. DMSO was a product of Lugal (Ukraine) and contained 1% water as an impurity. This amount was taken into account in the preparation of respective mixed solutions. All other chemicals were from Reakhim (Russia), of the highest purity available, and used as received. Doubly distilled water was used throughout.

The α-CT samples for the DSC experiments were prepared at concentrations of 1 to 2 mg/ml, by dissolving it either in phosphate (pH 2.6) or borate (pH 8.1) 10^{-2} M buffer solutions, in addition containing 5×10^{-2} M NaCl. The α-CT stock solutions for kinetic measurements, at a concentration of 1 mg/ml, were prepared in 10^{-3} M HCl (pH 3) and appropriate portions of 5 μl were added to the work solutions of total 5 ml (containing ATEE) to initiate the catalytic process. For the purpose of Lineweaver–Burk (LB) analysis, the concentration of ATEE was varied within 10^{-3} to 10^{-2} M, while that of α-CT was normally fixed at 10^{-8} M. Kinetic experiments were run at pH 8.4, with working solutions containing 5×10^{-2} M NaCl (no buffer used). The concentration of titrant (NaOH) was 10^{-2} M. The buffer solutions containing different DMSO concentrations were prepared by mixing solutions containing zero and maximal (70% DMSO v/v) concentration of DMSO, with the pH values adjusted separately.

2.2. Differential scanning calorimetry

Micro-calorimetric measurements for temperature-induced melting (denaturation) of α-CT in buffered DMSO-water mixed solutions (vide supra), were performed with a couple of DASM-4A adiabatic scanning calorimeters (Biopribor, Russia) at a heating rate of 2 K/min. When the repetitive scanning was applied, the cooling rate was 1 K/min. The methodological aspects of the DSC technique have been described earlier [21,28]. One of our calorimeters was in its original state (used in combination with an ink recorder), while another instrument was integrated with a PCI-DAS1001 (Measurement Computing Corporation) interface unit, providing direct PC access. In the case of a hardware recording, the DSC traces were first digitized and then in both cases treated through the Origin-based home-made PC program, according to the procedure described below. Usually, from the recorded thermograms, the partial (excess) heat capacity of the dissolved protein ($C_{p(prot)}$) can be calculated at any temperature, according to the equation [21,28]:

$$\Delta C_{p(app)} = C_{p(prot)} m_p - C_{p(solv)} \Delta m_s \quad (1)$$

where $\Delta C_{p(app)}$ is the deviation of the recorded protein sample thermogram from the baseline curve, $C_{p(prot)}$ and $C_{p(solv)}$ are the partial heat capacities of the protein and solvent, respectively, m_p is the mass of dissolved protein, and Δm_s is the mass of replaced solvent. The calorimetric enthalpy of thermal melting, ΔH_{cal}, in uncomplicated cases (normally exhibiting an endothermic melting peak with a single transition temperature, T_m), can be approximately calculated according to:

$$\Delta H_{cal} = \int_{T_1}^{T_2} C_{p(prot)} dT \tag{2}$$

where T is the absolute temperature, and T_1 and T_2 are the temperatures that correspond to the start and completion of heat absorption due to thermal melting ($T_1 < T_m < T_2$). To define T_1 and T_2, usually the linear approximations for the $C_{p(prot)}$ drift outside the temperature range of protein melting (at $T < T_1$ and $T > T_2$) were applied. Unfortunately, for the series of mixed solutions with additives which concentrations are varied within broad ranges, the values of the parameters $C_{p(solv)}$ and Δm_s, are usually either unknown, or can be estimated only in a rough manner. Hence, the absolute values of $C_{p(prot)}$ in cases like ours are hardly deducible with a high accuracy. However, since the value of ΔH_{cal} calculated though Eq. (2) signifies the integrated area, it does not depend on the absolute value of $C_{p(prot)}$ (T). Hence, one can apply the zero-baseline-correction procedure for calorimetric melting curves without any loss of accuracy in determining ΔH_{cal} (in anyway an error due to the baseline correction emerges). This approach that allows for a rigorous comparative analysis of calorimetric data obtained for the series of mixed solutions of unknown properties, has been successfully applied in many noteworthy cases (see, e.g., Refs. [12,55–57]). Importantly, the results of our calorimetric studies in standard cases (with no DMSO added) deduced from the full-bodied analysis (through Eqs. (1) and (2)), were in a good agreement with the published data [14,21]. All other calorimetric melting curves (deemed as inaccurate solely regarding the absolute values of $C_{p(prot)}$) were zero-baseline-corrected in order to exclude any error due to the unknown parameters, $C_{p(solv)}$ and Δm_s, and then Eq. (2) was applied to determine ΔH_{cal} for each studied case. Figs. 1–3 (Subsection 3.1 below) depict the zero-baseline-corrected calorimetric melting curves obtained through the above-mentioned procedure.

It has been demonstrated earlier [58] that for a folding/unfolding pattern of α-CT, in general, the three-state model, Eq. (3) [23–25], is applicable:

$$N \overset{fast}{\Longleftrightarrow} U_R \overset{slow}{\Rightarrow} D_I \tag{3}$$

where N denotes the native (or native-like) folded state, U_R denotes the reversibly denatured state (nearly totally unfolded random coil), and D_I represents the irreversibly denatured (intrinsically misfolded–aggregated) state [9,23–26,58]. If the protein does not refold upon cooling to the room temperature, or the parameters ΔH_{cal} and/or T_m tend to depend on the temperature scanning rate, this is an indication of an overall thermodynamic irreversibility due to the presence of an essentially irreversible, typically slow, intra-molecular aggregation process with the involvement of perverted hydrophobic contacts developing after the first (fast and reversible) unfolding stage (see Eq. (3)) at elevated temperatures. Since, the latter process is to be exothermic [25,58], although regarded as relatively slow, at finite (realistic) temperature scanning (rising) rates, under the equilibrium conditions for a reversible $N \Longleftrightarrow U_R$ stage, a part of $\Delta H_{NU(true)}$ (that is the true transition enthalpy for this process) is turned off, leading to effective experimental values that are less than the true ones, $\Delta H_{cal(eff)} < \Delta H_{NU(true)}$ [25,56]. It has also been demonstrated that notwithstanding this complication, the DSC technique may serve as a powerful tool for the thermodynamic analysis of the protein's three state pattern, allowing for a deduction of both, the reversible and irreversible motifs and respective hidden parameters [23–25,58]. For systems in

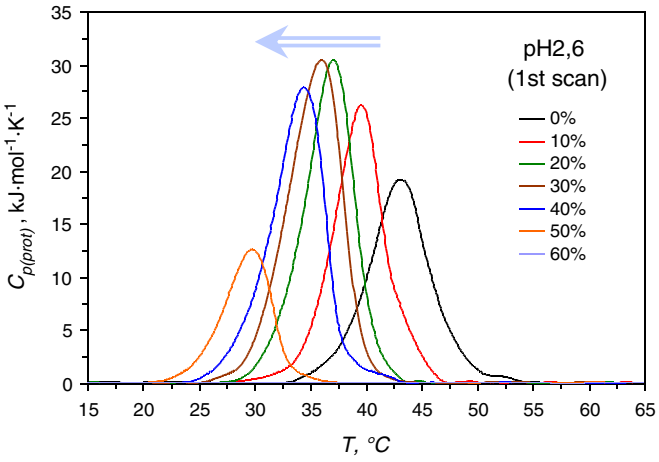

Fig. 1. First scanning DSC curves for the α-chymotrypsin thermal unfolding in the presence of 0–60% (v/v) DMSO concentrations, pH 2.6 (phosphate buffer), 0.05 M NaCl.

the present study, the folding reversibility and, seemingly the role of a second stage in Eq. (3), varied from experimental series to series and also within the series by variable [DMSO]. Actually, one of the important tasks of this work was to study the role of DMSO in both stages.

Let us consider how the presence of the irreversible step in Eq. (3) affects the parameters $T_{m(eff)}$ and $\Delta H_{cal(eff)}$, in more detail. The impact on $T_{m(eff)}$, in particular, should depend on the value of T_m (of the reversible step) itself and the degree of cooperativity of the irreversible step as well. In the case of azurin, e.g. [25], $T_{m(eff)}$ is rather high (81 to 86 °C) and, in addition, seemingly, the irreversible exothermic step is rather cooperative (yielding the peak-shaped negative profile). As a consequence, the resulting (mostly endothermic) peak is really distorted that becomes obvious through the appearance of the negative pit next to the positive peak [25]. In contrast, in our case (α-CT), T_m is much lower (falls within 30 to 53 °C), hence should be better separated from the exothermic step (supposed to be more pronounced at higher temperatures). In addition, in the present case, the exothermic step seems to be much less cooperative (much broader) since no negative pits were observed on thermograms throughout the experimental series (see Figs. 1 to 3 in the Subsection 3.1 below). Furthermore, for the series of experiments undertaken at pH 2.6 (in which the refolding pattern has been observed), all the values of T_m for the first and second scans throughout all samples coincided (see below). Because, as it has been proven for the representative sample with the 20% DMSO content, the restored peaks furthermore remain unaffected by repetitive multiple

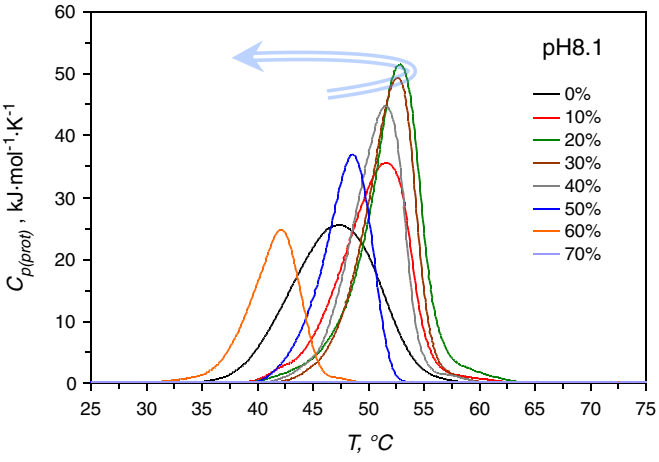

Fig. 2. First scanning DSC curves for the α-chymotrypsin thermal unfolding in the presence of 0–70% (v/v) DMSO concentrations, pH 8.1 (borate buffer) 0.05 M NaCl. The turnaround arrow indicates a changeover of the global stability trend with temperature.

scanning (vide infra), it automatically follows that the values of T_m, at least at pH 2.6, are totally unaffected by the irreversible step of exothermic aggregation. Importantly, our work seems to be the first systematic experimental effort towards the elucidation of a role of the irreversible step in the context of stabilizing/destabilizing impact of DMSO or any other organic additive on a globular protein. Similarly, the values of $\Delta H_{cal(eff)}$ for second scans at pH 2.6 remain unaffected by the further repetitive multiple scanning (Subsection 3.1), hence can be considered as the $\Delta H_{NU(true)}$ values. Consequently, one can safely conclude that all other values of $\Delta H_{cal(eff)}$ in the sequence of variable [DMSO], anyway, also reflect respective trends in $\Delta H_{NU(true)}$ for the $N \Leftrightarrow U_R$ process, at least semi-quantitatively. Finally, the values of $\Delta H_{cal(2)}$ for repeated scans (as compared to initial values due to first scans, ΔH_{cal}) should provide information on the degree of a protein refoldability upon the cooling (viz., on the role of the $U_R \quad D_I$ processes), when the case.

2.3. Kinetic studies of the catalytic activity

All kinetic (DPM) experiments were performed at 25 °C, exploiting the Radiometer Automatic Titration System RTS-822, according to the methodology described earlier [14,59,60]. In brief, the 5 ml cell was equipped with a PHC-4406 combined glass/calomel electrode and a water jacket supplied from the U-2 thermostat. Kinetic traces were recorded by means of the Radiometer Servograph REC-80, subsequently digitized and processed by PC. The values of maximal velocities, catalytic constants and Michaelis constants were calculated through the computerized LB analysis (for the representative graphs and numerical values, see Fig. 6 and Table 2 below).

The enzymatic activity of α-CT with respect to a specific ester substrate, ATEE, was examined in the presence of 0 to 70% (v/v) (0 to 10.5 M) DMSO. The overall catalytic pattern in this case can be expressed as [1,14,46,47,51,52]:

$$\begin{array}{ccccccc} & & k_1 & & k_2 & & k_3 & & \\ E + S & \underset{k_{-1}}{\Leftrightarrow} & ES & \Rightarrow & EA & \Rightarrow & E + P_2 \\ & & \Downarrow & & \Uparrow & & \\ & & P_1 & & H_2O & & \end{array} \qquad (4)$$

where E is the enzyme, S is the substrate, ES is a non-covalent enzyme–substrate complex, EA is an acyl-enzyme covalent intermediate, P_1 and P_2 are the ethanol and N-acetyl-L-tyrosine acid products, respectively, and k_1, k_{-1}, k_2 and k_3 are the rate constants of the individual reaction steps. The process in a steady-state regime obeys the Michaelis–Menten (MM) formalism in which the catalytic reaction rate, v, can be written as:

$$v = \frac{k_{cat}\ [S]_o\ [E]_o}{[S]_o + K_M}; \qquad v_m = k_{cat}\ [E]_o \qquad (5)$$

and

$$k_{cat} = \frac{k_2\ k_3}{k_2 + k_3}; \qquad K_M = \frac{k_{-1} + k_2}{k_1}\ \frac{k_3}{k_2 + k_3} \qquad (6)$$

where $[S]_O$ is the initial concentration of the substrate, $[E]_O$ is the total enzyme concentration, v_m is the maximal (saturation) reaction rate (at $[S]_O >> K_M$), K_M is the Michaelis constant, and k_{cat} is the catalytic constant. For the case of ATEE as a substrate, it was established that $k_2 >> k_3$ and $k_{-1} >> k_2$, and hence $k_{cat} \approx k_3$, and $K_M \approx K_S$ ($k_3 k_2$), where K_S is the equilibrium constant for the dissociation of the non-covalent enzyme–substrate complex. Furthermore, when $k_{cat} \approx const$ throughout the series of experiments at a fixed temperature, if the occurrence of the competitive inhibition is excluded (vide infra), the variability of K_M can be totally attributed to the variability of K_S. In Subsection 3.3 below, it will be demonstrated that the variable values of K_M (hence, of K_S) can be used as a measure of the active site flexibility in the presence of DMSO, urea and other effectors, within broad ranges of additive concentrations.

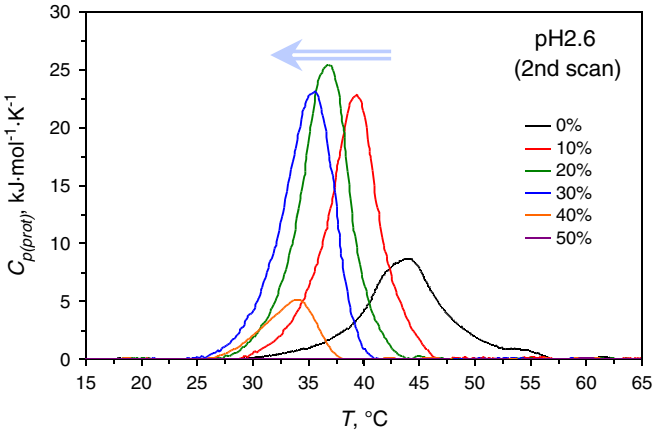

Fig. 3. (Compare with Fig. 1) Second scanning DSC curves for the α-chymotrypsin thermal unfolding in the presence of 0–50% (v/v) DMSO concentrations, pH 2.6 (phosphate buffer), 0.05 M NaCl.

One may question, whether the kinetic pattern of α-CT, in particular the pK_a values of catalytically important groups of the active center may be affected by DMSO. We observed the constancy of k_{cat} and gradual increase of K_M within the concentration range up to 25% (ca. 3.5 M) DMSO (see Subsection 3.2 below). Since our kinetic studies were performed at pH 8.4, if pK_a of catalytic imidazole group of His-57 was perturbed significantly (exceeding ±0.5 units), within the abovementioned DMSO concentration range, we should unavoidably observe some decrease of k_{cat}, what is not the case. Consequently, our results are not affected by any perturbation of pK_a (if any).

3. Results and discussion

3.1. Differential scanning calorimetry and the thermal melting pattern

Figs. 1 and 2 depict results of calorimetric studies for temperature-induced denaturation (melting) of α-CT in the absence and presence of variable DMSO concentrations, in acidic (pH 2.6, phosphate buffer) and weakly alkaline (pH 8.1, borate buffer) environments, respectively. Depicted curves represent the zero-baseline-corrected temperature dependencies for a partial heat capacity of α-CT throughout the initial (first) calorimetric scans, whereas Fig. 3 depicts similar curves (taken at pH 2.6) for the repeated (second) calorimetric scans (vide infra). Figs. 4 and 5 show dependencies of the parameters T_m and ΔH_{cal} on the DMSO concentrations applied. The thermal melting process of native-like forms of α-CT (unperturbed by DMSO) is known to exhibit a single endothermic peak which characteristics, viz., T_m and ΔH_{cal}, were found to be in a good agreement with literature data obtained under comparable conditions [14,21]. Figs. 1 to 3, along with Figs. 4 and 5, demonstrate that upon variation of the DMSO concentration, the zero-baseline-corrected thermograms and the respective extracted parameters exhibited mostly non-monotonic behavior. Table 1 summarizes the numerical values for these parameters.

At pH 2.6, upon variation of the DMSO concentration up to 50% (v/v), T_m decreased monotonically until the disappearance of a characteristic peak at 60% DMSO. At the same time, the value of ΔH_{cal} displayed a more complex behavior, exhibiting the weakly pronounced maximum around 25% DMSO (v/v) , followed by a further decrease until its disappearance. This behavior is very similar to that of lysozyme at pH 3 [61], pH 5 and pH 7 [62], with the only difference that plots of T_m vs. [DMSO] were reported to be linear instead of curved as in our case (Fig. 4). Furthermore, the maximum for ΔH_{cal} vs. [DMSO], although it also occurs in the same range of [DMSO], is somewhat more pronounced in the present case. Remarkably, the reversibility of protein unfolding, i.e. the

ability to restore the initial (native-like) conformation upon gradual cooling (as tested by performing repeated calorimetric scans, see Fig. 3), initially amounting to ca. 54%, increased notably in the presence of DMSO. In particular, in the case of 20% DMSO, the reversibility increased to ca. 75% (regarding the value of ΔH_{cal}). Furthermore, this degree of reversibility was preserved upon repetitive 6-times DSC scanning within 24 h. Actually, the role of DMSO as a molecular chaperon has long been recognized [35,43–45].

At pH 8.1, the impact of the variable DMSO concentration was to some extent similar to that at pH 2.6, but still rather divergent. In particular, whereas ΔH_{cal} exhibited a similar smooth maximum at 30% DMSO regarding the dependence on [DMSO] (Fig. 5), in contrast to the case of pH 2.6, T_m also exhibited a very smooth maximum around 20 − 30% DMSO (v/v) (Fig. 4), which, in overall, indicates a comparable stabilization impact through ΔH_{cal} but less destabilizing impact through ΔS_{cal}, leading to the global stabilization through T_m (ΔG_{cal}) (implying the first scan pattern and not the chaperoning effect upon repetitive scanning). However, in line with other discrepancies vs. the case of pH 2.6, the refoldability has not been detected, neither in the absence, nor at any concentration of DMSO.

Partially diverse behavior of α-CT at pH 2.6 and pH 8.1 regarding the impact of DMSO allows for a thorough analysis of factors that determine thermodynamic patterns of this globular protein. Obviously, at least two mechanisms are involved. One of them, that is stabilizing and mostly of enthalpic nature, is responsible for the appearance of a smooth maximum for ΔH_{cal} vs. [DMSO] at ca. 25 − 30%, within the concentration range of 0 < [DMSO] < 50% (v/v). Most importantly, Arakawa et al. [63] demonstrated that the preferential interaction of DMSO with various proteins including chymotrypsinogen, CTG (a biological precursor of α-CT) and lysozyme (the reference enzyme), within this DMSO concentration range, is negative (compared to the positive one for water) exhibiting a smooth minimum around 30% DMSO (v/v). The mechanism behind both these motifs seems to be the same, and common for at least all respectively studied globular proteins, and to some extent, for many hydrophobic additives, e.g. alcohols (see, e.g., Refs. [64–67]). Indeed, the addition of 4.5 M methanol resulted in a smooth maximum for ΔH_{cal} vs. [methanol] in the case of lysozyme [64], very similar to the impact of 4.5 M (30% v/v) DMSO on lysozyme [61,62] or α-CT (this work).

According to spectroscopic [36,68–70] and computational [71,72] studies, within the concentration range 0 < [DMSO] < 50% (with a minor variation), proteins in a global context, mostly attain native-like conformations (vide infra). The negative preferential solvation by DMSO that has been observed throughout this range [63], automatically implies positive preferential solvation by water molecules. No doubt, the stabilizing enthalpic component reflected by the non-monotonic behavior (smooth maximum around 25 − 30% DMSO) for ΔH_{cal}, is caused by strengthening of the water–protein and water–water hydrogen bonding within the protein hydration layer that anyway (implying the native-like states) directly contributes to the protein stabilization (vide infra).

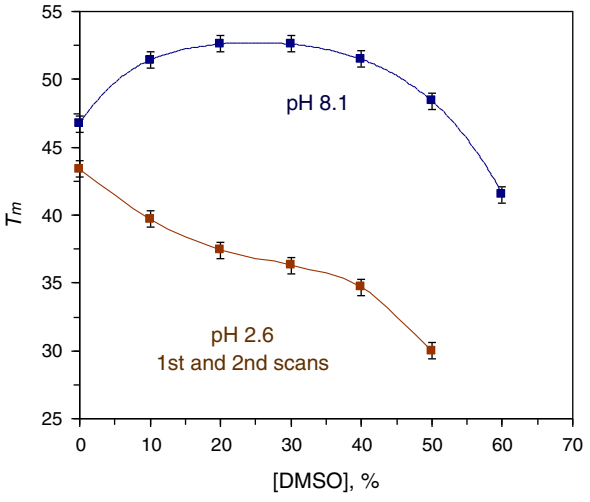

Fig. 4. Dependencies of the transition temperatures for the temperature-induced denaturation of α-chymotrypsin on the DMSO concentration at pH 8.1 (above) and pH 2.6 (below). See text for the experimental details.

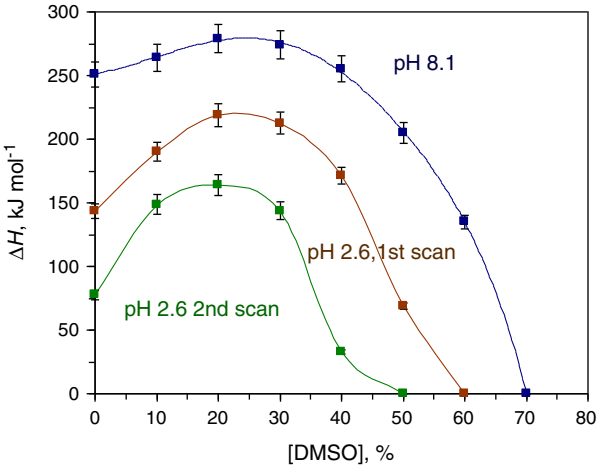

Fig. 5. Dependencies of the calorimetric enthalpies for temperature-induced denaturation of α-chymotrypsin on the DMSO concentration at pH 8.1 (top) and pH 2.6 (first and second scans, mid and below, respectively). See text for the experimental details.

In contrast to the above considered concentration range, above ca. 50% DMSO, a dramatic drop in the values of T_m and ΔH_{cal} occurred, followed by eventual peak disappearance around 60–70% DMSO, depending on the solution pH (Figs. 1 to 5 and Table 1). According to Arakawa et al. [63], above ca. 50% DMSO, a region of positive preferential solvation of proteins by DMSO starts to rise. The extent of the "positive" DMSO–protein interaction in this segment, unlike the region of the "universal" ("negative") interaction within 0 < [DMSO] < 50% [63], is largely specific regarding the protein's "personality". It is natural to propose that at higher concentrations of DMSO, it starts to displace water molecules from proteins' interfacial regions (vide infra). In addition, because of their prevailingly hydrophobic nature, DMSO molecules tend to preferentially stabilize the unfolded state of α-CT, thanks to extensive interactions with exposed hydrophobic groups. Obviously, within the DMSO concentration range of 50 to 60/70% (v/v), the α-CT structure becomes largely destabilized by the disposal of an increasingly large number of DMSO molecules on its surface and, in addition, in the course of the temperature-induced melting, onto the increasingly solvent-exposed hydrophobic groups. Above 60% DMSO at pH 2.6 and 70% DMSO at pH 8.1, and room temperature, α-CT seemingly attains a totally denatured conformation (see, however, Subsection 3.3 for further discussion).

Table 1
Thermodynamic parameters for the thermal unfolding of the α-chymotrypsin in the presence of different DMSO concentrations in borate buffer, pH 8.1 and first and second scans in phosphate buffer, pH 2.6 (0.05 M NaCl). Experimental errors are ca. 10% and 1%, for ΔH_{cal} and T_m, respectively.

		pH 8.1		pH 2.6, 1st scan		pH 2.6, 2nd scan	
[DMSO], vol.%	[DMSO], mol/l	T_m, °C	ΔH_{cal}, kJ mol^{-1}	T_m, °C	ΔH_{cal}, kJ mol^{-1}	T_m, °C	ΔH_{cal}, kJ mol^{-1}
0	0	46.7	251	43.4	144	43.3	78
10	1.5	51.4	264	39.7	190	39.8	149
20	3.0	52.6	279	37.4	219	37.6	164
30	4.5	52.6	274	36.3	213	36.5	144
40	6.0	51.5	255	34.7	171	34.5	33
50	7.5	48.4	205	30.0	69	–	0
60	9.0	41.5	135	–	0	–	0
70	10.5	–	0	–	0	–	0

3.2. The Lineweaver–Burk pattern for a catalytic activity

Fig. 6 depicts some results of kinetic studies for the enzymatic hydrolysis of a specific ester substrate, ATEE by α-CT at pH 8.4, 0.05 M NaCl (no buffer), in the presence of variable DMSO concentrations. In particular, the LB plots are depicted for cases of DMSO concentrations from 0 to 25% (v/v) where the catalytic constant remained virtually unaltered (note the common intercept of the linearized dependencies). Above 25% DMSO, k_{cat} started to decrease and became non-measurable at 70% DMSO where also the DSC melting peak disappeared (vide supra). At the same time, the value of K_M increased almost monotonically throughout, until the eventual full denaturation occurred at 70% DMSO. Table 2 depicts all the values obtained for k_{cat} and K_M (note the rapid increase of experimental error above 40% DMSO).

It can be mentioned that the LB pattern displayed in Fig. 6 is formally compatible with a mechanism of simple competitive inhibition by high concentrations of DMSO (for the inhibitory classifications, see, e.g. [1]). As mentioned in the Experimental section, for the system under study, the Michaelis constant is proportional to, and mainly representative of, the equilibrium constant, K_S, for the dissociation of the enzyme–substrate non-covalent (precursor) complex [1,14,46,47,51–54]. The mechanism of competitive inhibition implies binding of the inhibitor species to single (or several) position(s) of the enzyme active site to temporarily block it (them) against specific substrate binding. In such cases K_S (hence, K_M) gradually increases while k_{cat} remains unchanged [1,14]. However, a careful combined analysis of our current results and earlier findings [14,15], together with the previous basic deductions encompassing structural aspects for the interaction of α-CT either with polypeptide-like inhibitors (disclosed via the X-ray studies) [73–75], or extended polypeptide substrates (revealed through the specific series of kinetic data) [75–77], respectively, allowed us for much more advanced insights. Indeed, the impact of DMSO on the LB pattern within the concentration range of 0–3.75 M (0–25% v/v; Fig. 6), is very similar to that of urea within the concentration range of 0–6 M [14,15]. Urea is known to be a moderate denaturant that causes totally destabilizing effects on the global conformation of globular proteins [78–82]. Specifically, for the case of α-CT, our previous studies [14,15] (see also Refs. [66,67,80]) indicated that ΔH_{cal} decreased almost gradually within the same range of [urea].

Furthermore, one should notice that α-CT is an enzyme that is designed to interact with, and to cleave polypeptide substrates. Based on the abovementioned X-ray-structure-based results, the interaction scheme for the α-CT active center and natural (long) polypeptide substrates has been proposed implying that the substrate moiety forms antiparallel β-structures with respective (mostly exposed) peptide motifs of the enzyme active site, extending to both sides of the scissile bond [73–77]. This scheme naturally considers multipoint, energetically favorable interactions of both, the complementary backbones (viz., the peptide bond moieties interacting through the hydrogen bonds) and complementary side-chains (viz., the non-polar moieties interacting through the hydrophobic forces). For α-CT, a number of hydrophobically interacting positions within the active site crevice may amount to 6–7 (extending over 18–21 Å) [73–77]. Involvement of longer polypeptides as substrates, seemingly, provides enhanced multipoint interaction favoring the improved "induced fit" and much more efficient catalysis, presumably through the combined cooperative/allostery-like regulation mechanism [1,2,4,10,13,16]. On the other hand, the synthetic substrates like ATEE, may occupy only a few (namely 3; although most important) of respective likely positions [47]; hence leaving other potentially binding (apolar or polar) exposed subsites free for the interaction with water or organic additives. Obviously, networks of water molecules situated within or near the active site crevice (at times residing at the "empty" positions, free of the ATTE molecule), because of the irregularly chained structure (low cooperativity), cannot favor the maximal catalytic effect via the allostery-like interaction. This picture is in contrast to one for interfacial waters belonging to compactly folded ("structure supporting") domains. These parts of α-CT, like in other globular proteins, have mostly polar and charged groups exposed to the solvent [1] that favors formation of highly cooperative aqueous chains and networks (vide infra).

The very similar LB patterns of α-CT with the DMSO (this work) and the urea additives [14,15], which have dissimilar, prevailingly non-polar (hydrophobic, viz., 2× $-CH_3$ vs. =O) and polar (hydrophilic, viz., 2× $-NH_2$ and =O) moieties in their structures, respectively, furthermore points to: (a) the entirely nonspecific character of an impact for either of these two additives, presumably via the multi-point weak interaction within the active site region (crevice); and (b) that respective positions, although supposed to be dissimilar (apolar and polar, respectively), should be structurally interconnected to cause similar negative impact (through the increase of K_M vide infra). Consequently, nonspecific, totally noncooperative, weak interaction either with the side chains (DMSO; through hydrophobic binding), or backbone moieties (urea; through the hydrogen bonding) of polypeptide-shaped counterpart motifs situated within the active site crevice of α-CT can be deduced. The fact that the active site solvating waters of α-CT (and, seemingly, of other soluble enzymes, as well), in the absence of substrates, cannot form really cooperative (energetically favorable) interfacial chains and/or networks, obviously, is dictated by the requirements for: (a) a sufficiently high flexibility of the entire active site; and (b) the minimization of acting water molecules as competitive inhibitors. Clearly, weakly interacting, small organic additives like DMSO or urea, having low affinity (comparable with that of water) to respective positions within the active site cleft, cannot seriously compete with specific substrates of

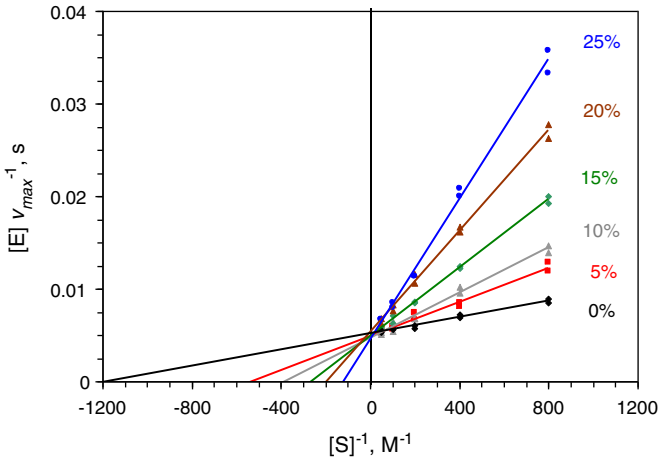

Fig. 6. Lineweaver–Burk plots for the ATEE hydrolysis by α-chymotrypsin in the presence of various concentrations of DMSO; pH 8.5, 0.05 M NaCl, 25 °C.

Table 2
Kinetic parameters for hydrolysis of ATEE with α-chymotrypsin in the presence of different DMSO concentrations (pH 8.5, 0.05 M NaCl, 25 °C). Experimental errors are ca. 10% and 20% below and above 40% DMSO, respectively.

[DMSO], vol.%	[DMSO], mol/l	K_M, M^{-1}	k_{cat}, s^{-1}
0	0	8.2×10^{-4}	205
10	1.5	2.4×10^{-3}	210
20	3.0	5.4×10^{-3}	200
25	3.75	8.3×10^{-3}	214
30	4.5	1.5×10^{-2}	150
40	6.0	2.2×10^{-2}	136
50	7.5	2.0×10^{-2}	44
60	9.0	2.5×10^{-2}	36
70	10.5	–	–

any length, e.g., with ATEE. On the other hand, the ATEE molecule seems to be too "short" either to stabilize the active site of α-CT by itself, or to prevent unoccupied positions against the noncooperative (hence destabilizing) multi-positional interaction with DMSO or urea. One should note again that the maximal catalytic efficiency should require the excellently tuned conformational balance for the achievement of a "perfect induced fit" [1,2,4,10,13,16].

The finally deduced picture, where the "inhibitor" (DMSO or urea), like water, may bind very weakly to multiple positions the number of which, at least, 2 to 3 times exceeds one for the substrate's (ATEE's) binding groups, has little to do with a "classical" scheme of competitive inhibition. Thus, it seems that the reason behind the appearance of the distinct LB pattern depicted in Fig. 6 and found in Refs. [14,15], should be sought elsewhere.

3.3. Dual impact of DMSO regarding the global and local stability/flexibility and function of α-CT

So, if there is little, if any, contribution due to the competitive inhibition by DMSO (and urea, see Refs. [14,15]), then what is the reason for a characteristic LB pattern (gradual increase of K_M at constant k_{cat}) portrayed in Fig. 6 (and by a similar figure: "Fig. 2" in [14])? We propose that the reason is a gradual increase of the active site flexibility (decrease in its local stability) caused by multipoint weak DMSO–protein (or urea–protein [14,15]) interactions around the active site. In this context, it seems expedient to evoke data of Timasheff et al. for the preferential interaction of DMSO [63] and urea [78] with proteins. Preferential interaction with urea seems to be positive for all the globular proteins throughout, including both, native-like and unfolded/denatured states [78], whereas for DMSO, within the concentration range of 0–50% (v/v) (up to 7.5 M) it is negative, however, changes to a positive type above this point and exceedingly increases thereafter, especially for the case of CTG [63]. However, the negative preferential interaction at lower concentrations of DMSO does not mean its total exclusion from the protein surface. Indeed, according to the same paper [63], notwithstanding the negative preference, actual binding of DMSO to CTG and other globular proteins takes place starting from the lowest concentrations and increases dramatically above 50% (v/v), especially for the case of CTG. This result is in a good agreement with those of several structural [83] and computational [71,72] studies that report on the existence of DMSO binding positions at the protein's interfacial regions, especially near the active sites that are rich of both, polar and non-polar loci (vide supra).

Importantly, according to [63], roughly 20 molecules of DMSO, at the bulk concentration of 20–30% (v/v), associated with CTG (presumably also with α-CT) can be deduced. This number increases to ca. 60 to 70 at a DMSO bulk concentration of 40–50%. In light of the computational work in the cases of subtilisin [71] and lysozyme [72], it is logical to suppose that a number of DMSO molecules weakly associated around the α-CT flexible area (active site), within the range $10 < c < 50\%$ (v/v), initially amounts at least to ca. 6–7 and increases to ca. 20. Indeed, the parameter K_M (or K_S) has long been recognized as a measure of the active site flexibility (being an inverse merit for the rigidity, i.e., stability) that can be altered by addition of denaturants/stabilizers [13,15,84], by biological evolution [53,54], or simply by temperature [15,51,52]. Furthermore, on the basis of X-ray [85,86] and combined inactivation/denaturation studies [1–6,14,15,48–50], it has been proposed that proteins' active sites retain much more flexible constitution compared to more rigid (compact) supporting platforms. On the other hand, for the case of DMSO as a representative additive of multilateral nature, it has been proposed that it's binding to different parts of proteins, may cause either local stabilizing, or local destabilizing effects [35,36,63,72]. Our data suggest that DMSO within $0 < c < 50\%$ (v/v), in weakly alkaline solutions (pH 8.1–8.4), has a stabilizing impact on the protein's global conformation (implying that its non-functional compact area serving as a supporting platform) and a destabilizing impact on the protein's local conformation (implying that its active site inherently possesses high flexibility, allowing for effective functioning).

Since DMSO, seemingly has a significant impact on the local stability/flexibility of α-CT, implying its catalytically active site (vide supra), it is crucial to consider the actual mechanism behind this impact. For the case of ATEE as a substrate, in discrepancy with our result, Eremeev [47] found that the value of k_{cat} was decreasing within $0 < [\text{DMSO}] < 25\%$ (v/v), whereas K_M behaved in a manner that was similar to our case (i.e., increasing). However, in that work, the $CaCl_2$ additives at 10^{-2} M were applied throughout [47]. The Ca^{2+} ions are well-known to bind specifically to many globular proteins including α-CT [87–90], affecting the catalytic properties dramatically [14,89]. Since, direct comparison of these two sets of results is not straightforward. Nevertheless, in Ref. [47], for substrates for which case the acylation step (k_2, Eq. (4)) is rate determining, some activation effect via the increase of k_{cat}, has been observed (within the same concentration range of DMSO). If the same side effect due to the presence of Ca^{2+} is implied, the "true" activation effect of DMSO in that case can be even more pronounced. According to some preceding and more recent work [1–6,8,13,16–20], biomolecular, in particular, enzymatic processes, in general, can be categorized as: (a) those strongly contributed by the conformational coordinate, i.e., requiring energy-consuming rearrangements of the protein's active site (flexible area), and (b) those which are mostly controlled by the chemical transformations (perfect induced fit). In the former case some destabilization (flexibilization) of the active site may facilitate increase of the catalytic effect (see Refs. [40,47], e.g.), while in the latter case k_{cat} may remain unaltered or decrease (this work and Refs. [12,14,59,60]).

3.4. Impact of DMSO regarding the global destabilization, chaperon effect and molten globule state

It has been deduced earlier that in unfolded states of globular proteins, DMSO molecules mostly interact with solvent-exposed hydrophobic groups, which in native-like states are mostly hidden inside proteins' interiors, to mutually interact and form compact hydrophobic cores [1,91,92]. This condition accounts well, on the one hand, for the destabilizing effect of high concentrations of DMSO, preferably interacting with hydrophobic side groups in unfolded state and, on another hand, for the protective (chaperoning) properties of DMSO against protein aggregation in an unfolded state (see Eq. (1) in Subsection 2.3 above). The regenerative effect of DMSO does not work in weakly alkaline media, closer to the isoelectric point of α-CT (8.76) [93], seemingly because almost all the ionizable groups are charged, favoring formation of more strongly hydrogen-bounded water networks also in the denatured (unfolded) state, thus facilitating aggregation (perverted association) of hydrophobic groups even in the presence of excess DMSO concentrations. In contrast, at pH 2.6 where virtually all the negative charges of the solvent-exposed carboxylic groups are neutralized, the repulsive interaction between positively charged amino groups facilitates a more expanded character of the unfolded state, weakening of the connecting hydrogen-bonded aqueous networks, and a better access of DMSO molecules to the exposed hydrophobic side-groups. Importantly, in contrast to the case of pH 8.1, partial refolding of α-CT at pH 2.6 was observed even in the total absence of DMSO additives (Table 1). In that case, DMSO acting as a molecular chaperon notably improved the refolding ability.

Returning now to our data depicted in Figs. 1 to 5 and Table 1, we will attempt to elucidate further the mechanism behind the complex behavior of ΔH_{cal}, namely the appearance of a smooth maximum around 25 − 30% DMSO (v/v) at both pH values, and of a similar maximum for T_m at pH 8.1. In light of the discussion given in the subsection above, the first increase in ΔH_{cal} can be explained by the negative preferential solvation of α-CT by DMSO (hence the positive preferential solvation by water). This effect is common for additives (like sugars, polyols) that stabilize globular proteins largely through the

exclusion of the aqueous phase from the bulk, leading to a compactization (contraction) of the water layer at the protein surface [80,94]. Seemingly, this is also true for the case of DMSO within $0 < c < 50\%$ (v/v). In the context of the above mentioned details, the possible role of the protein's solvent-exposed charge groups in the stabilization of native-like states should be mentioned as well. In general, the thermodynamic stability of globular proteins is much higher at neutral pH (more precisely, under the protein's isoelectrical condition), compared to the acidic or alkaline pH's [21,92,95–97]. The classical model of Privalov et al. [21,22] explains this fact via the dependence of ΔH_{cal} solely on T_m, not on pH (see also Refs. [95,96]). This is because the classical model assumes that the enthalpy contribution, stabilizing the native state over the unfolded state, emerges solely from intra-globular interactions, not from solvation effects, specifically, not from the difference of solvent-exposed charged group arrangements (difference in mutual separations, e.g.) for these two states [21,22,95,96,98,99]. Disregarding the latter factor (vide infra) automatically leads to the independence of ΔH_{cal} (that, inter alia, also results from the enthalpy of solvation, ΔH^{O}_{solv}) of the surface charge distribution (pH). We consider this deduction as an oversimplification since the solvent-exposed oppositely charged groups [100–104] capable of forming the strongly hydrogen-bonded aqueous chains and networks [105–108], are situated much closer in native states [109], hence are much more stabilized through the respective enthalpy contribution (certainly, at some unfavorable entropy cost) [105,106,110,111]. Close to the isoelectric point, the oppositely charged surface-exposed groups of the native protein (see, e.g., Refs. [100–104]) are situated much closer to each other, compared to the unfolded state(s), thus facilitating formation of very strong hydrogen-bonded aqueous bridges/networks [105,106] that also appear even in the common liquid water, however, in a minor fraction [110,111].

Indeed, according to the extended statistical analysis by Wada and Nakamura [109], in addition to the solvent-exposed "normal" (contact) ion-pairs of native globular proteins that are on average separated by ca. 4–5 Å (deemed as to contribute little to the stability [91,105,98–102]), there is a remarkable fraction of oppositely charged ionic groups separated by ca. 6–10 Å [109]. This is exactly the distance range suitable for the formation of strongly hydrogen-bonded aqueous bridges involving 1–2 water molecules, consequently, of networks capable of a strong enthalpy contribution to the native state stability [101,102,108,109]. Certainly, hydrogen-bonded aqueous networks (forming so called bound water [96]) are formed in any way through the interaction with uncharged, yet polar interfacial groups, both in native-like (although destabilized) and unfolded states (respective aqueous chains can encompass more than just two water molecules, and may be involved in anomalous superficial proton conductivity [105,106]). Together with other energy/entropy contributions (intra-globular hydrogen-bonding, hydrophobic solvation, configuration entropy [21,22,98,99]), the excess stabilization/destabilization is achieved through a delicate altering of the balance between the pH-responsive surface-exposed charged states and the respective effective distances between them [98,99,102,104]. Furthermore, if the strongly hydrogen-bonded aqueous layer (network) contributes notably towards the stabilization of native-like states (vs. unfolded states), through the favorable enthalpic stabilization caused by closer placement of oppositely charged solvent-exposed charged groups (vide supra), additional stabilization through this enthalpic term becomes easily understandable through a mechanism of bulk water exclusion and, thus, its additional attraction by the interfacial charged/polar groups (preferential hydration). This would lead to more compact and stable water networks, with a larger contribution to the solvation enthalpy. This contribution although strongly underestimated in the past, in light of recent findings [102,106,108,109,112–114] seems to be rather "universal" and a crucial factor for globular proteins. For α-CT, in particular, our data enables the tentative estimate of this contribution that may amount to at least ca. 30–50% of the resulting value of ΔH_{cal} (in the absence of the DMSO or other additives; work in progress).

We now again consider the dramatic drop in values of T_m and ΔH_{cal} above ca. 50% DMSO, followed by the eventual peak disappearance around 60–70% DMSO, depending on the solution pH (Figs. 1 to 4 and Table 1). According to the data on the preferential solvation of a number of globular proteins [63], and results of several spectroscopic (NMR, CD, etc.) studies for lysozyme [36,68,69], within the region 50 to 70% DMSO (v/v), proteins attain intermediate global conformations between the native-like and unfolded (denatured) states, that are characteristic for the "molten globule" states originally disclosed for low pH solutions [27,115–118]. These states are still compact and native-like, however, in overall, retain much higher fluctuational mobility [14,15,27,115–118]. The DSC melting curves for these kinds of states gradually shift to lower temperatures, broaden and display lower values of calorimetric enthalpies [14,15,117,118]. This is what we observed in our DSC experiments at the DMSO concentrations exceeding ca. 50% (v/v). In addition, it should be mentioned that the disappearance of the DSC peak in some cases does not mean total denaturation of a given protein. In distinct cases the compact molten-globule-like configurations have been detected even in the absence of a characteristic melting peak; however, the characteristic step in $C_{p(prot)}$ can be visible [14,15,117,118]. In the present work, no steps for $C_{p(prot)}$ were observed at DMSO concentrations of 50% (pH 2.6) and 60% (pH 8.1), whereas steps were detected within 0 to 40–50% DMSO, respectively (not shown here). This can be an indication that before the *T*-induced transition (melting) occurs, the interfacial water network of α-CT is already essentially destroyed, and after the transition (to the denatured state) the newly solvent-exposed hydrophobic groups mostly interact with the DMSO molecules, rather than with water.

4. Conclusions

The impact of DMSO on the functional and unfolding patterns of α-CT turned out to be dualistic in three different ways. In particular:

1. Within the concentration range of 0 to 50% (v/v), the impact of DMSO on the global conformation of α-CT (implying its compact — "structure-supporting" area) is, in overall, either stabilizing (pH 8.1) or destabilizing (pH 2.6). However, the calorimetric enthalpy displays a smooth maximum indicating the stabilizing contribution in both cases.
2. Within the same concentration range, the impact of DMSO on the local conformation of α-CT (implying its flexible area — the active site), as judged on the grounds of a LB outline, is destabilizing.
3. Within the concentration range of 50 to 70% (v/v), the DSC patterns of α-CT exhibit a behavior that is characteristic for the molten-globule-like states; followed by the full denaturation at higher concentrations of DMSO.
4. Regarding the global stability pattern, the interplay of observed effects most probably can be ascribed to: (a) the negative preferential solvation of DMSO within 0 to 50% (v/v), and respective strengthening of a hydrogen-bonded water network at the interface of α-CT (covering the structure-supporting area); and (b) the positive preferential solvation of DMSO above 50%, and the intensified binding of DMSO molecules to the particular surface-exposed non-polar groups (in the native-like state) and the newly exposed hydrophobic side groups (in the denatured state).
5. Regarding the local stability (flexibility), the observed kinetic pattern can be realistically explained by the different distributions of particular solvent-exposed non-polar and polar groups within and around the active site crevice (flexible area) of α-CT. In particular, by evoking the fact that the local substrate binding positions are nothing else than the side-chain and backbone moieties of polypeptide motifs that are complementary to the natural polypeptide substrate. For cases of short (less specific) synthetic substrates like ATEE, the unoccupied apolar or polar positions are exceedingly open for the interaction with partially hydrophobic (DMSO) or hydrophilic (urea)

effectors that can readily destabilize active site through the multipoint yet non-cooperative interactions.

6. Regarding the global pattern, seemingly, there is a strong enthalpic contribution to the excess stability of native vs. unfolded states of globular proteins, emerging from more favorable electrostatic interaction of oppositely charged surface groups connected through the strong hydrogen-bonded aqueous chains. This interaction seemingly is strengthened upon the addition of up to 25–30% DMSO (v/v), thanks to the water exclusion from the bulk solution (i.e., the positive preferential solvation of α-CT by water).
7. Our findings open new prospects for the selective and fine tuning of both, the enzyme's local and global stability, and flexibility and, ultimately, the function through the application of small organic additives, such as DMSO.

Acknowledgments

Research grants from the Volkswagen Foundation, Germany (I/83 395), Rustaveli National Science Foundation, Georgia (no. 11/14/2012) and the Deutsche Forschungsgemeinschaft, Germany, are kindly acknowledged. We are thankful to Dr. L. Kukutaria for his expert work towards the modification of a DASM-4A instrument and writing the respective PC program. Dr. E. Kiziria is acknowledged for expert diverse technical help, and Dr. N. Shengelia is acknowledged for her laboratory assistance.

References

[1] A.R. Fersht, Structure and Mechanism in Protein Science: A Guide to Enzyme Catalysis and Protein Folding, 2nd ed. Freeman, New York, 1998.
[2] M. Wolf-Watz, V. Thai, K.A. Henzler-Wildman, G. Hadjipavlou, E.Z. Eisenmesser, D. Kern, Linkage between dynamics and catalysis in a thermophilic–mesophilic enzyme pair, Nature Structural & Molecular Biology 11 (2004) 945–949.
[3] Q. Shu, C. Frieden, Relation of enzyme activity to local/global stability of murine adenosine deaminase: ^{19}F NMR studies, Journal of Molecular Biology 345 (2005) 599–610.
[4] K. Teilum, J.G. Olsen, B.B. Kragelund, Protein stability, flexibility and function, Biochimica et Biophysica Acta 1814 (2011) 969–976.
[5] A.N. Morozov, D.C. Chatfield, Chloroperoxidase-catalyzed epoxidation of cis-β-methylstyrene: distal pocket flexibility tunes catalytic reactivity, Journal of Physical Chemistry B 116 (2012) 12905–12914.
[6] Z. Amini-Bayat, S. Hosseinkhani, R. Jafari, K. Khajeh, Relationship between stability and flexibility in the most flexible region of *Photinus pyralis* luciferase, Biochimica et Biophysica Acta 1824 (2012) 350–358.
[7] J.N. Onuchic, H. Nymeyer, A.E. Garcia, J. Chahine, N.D. Socci, The energy landscape theory of protein folding: insights into folding mechanisms and scenarios, Advances in Protein Chemistry 53 (2000) 87–152.
[8] A. Warshel, W. Parson, Dynamics of biochemical and biophysical reactions: insight from computer simulations, Quarterly Reviews of Biophysics 34 (2001) 563–679.
[9] C.M. Dobson, Protein folding and misfolding, Nature (London) 426 (2003) 884–890.
[10] O. Miyashita, J.N. Onuchic, P.G. Wolynes, Nonlinear elasticity, proteinquakes, and the energy landscapes of functional transitions in proteins, Proceedings of the National Academy of Sciences of the United States of America 100 (2003) 12570–12575.
[11] J.N. Onuchic, P.G. Wolynes, Theory of protein folding, Current Opinion in Structural Biology 14 (2004) 70–75.
[12] D.E. Khoshtariya, T.D. Dolidze, S. Seyfert, D. Sarauli, G. Lee, R. van Eldik, Kinetic, thermodynamic and mechanistic patterns for free (unbound) cytochrome *c* at Au/SAM junctions. Impact of electronic coupling, hydrostatic pressure, and stabilizing/denaturing additives, Chemistry - A European Journal 12 (2006) 7041–7056.
[13] M. Shushanyan, D.E. Khoshtariya, T. Tretyakova, M. Makharadze, R. van Eldik, Diverse role of conformational dynamics in carboxypeptidase A-driven peptide and ester hydrolyses. Disclosing the "perfect induced fit" and "protein local unfolding" pathways by altering protein stability, Biopolymers 95 (2011) 852–870.
[14] D.E. Khoshtariya, M. Shushanian, R. Sujashvili, M. Makharadze, E. Tabuashvili, G. Getashvili, Enzymatic activity of α-chymotrypsin in the urea-induced molten-globule-like state: a combined kinetic/thermodynamic study, Journal of Biological Physics and Chemistry (Basel) 3 (2003) 2–11.
[15] M. Shushanyan, R. Sujashvili, E. Tabuashvili, M. Makharadze, G. Getashvili, D.E. Khoshtariya, Kinetic and thermodynamic manifestations of thermally induced molten-globule-like state of α-chymotrypsin, Journal of Biological Physics and Chemistry (Basel) 6 (2006) 51–55.
[16] K.A. Henzler-Wildman, V. Thai, M. Lei, M. Ott, M. Wolf-Watz, T. Fenn, E. Pozharski, M.A. Wilson, G.A. Petsko, M. Karplus, C.G. Hübner, D. Kern, Intrinsic motions along an enzymatic reaction trajectory, Nature (London) 450 (2007) 838–844.
[17] A.V. Pisliakova, J. Caoa, S.C.L. Kamerlina, A. Warshel, Enzyme millisecond conformational dynamics do not catalyze the chemical step, Proceedings of the National Academy of Sciences of the United States of America 106 (2009) 17359–17364.
[18] D.E. Khoshtariya, J. Wei, H. Liu, H. Yue, D.H. Waldeck, The charge-transfer mechanism for cytochrome c adsorbed on nanometer thick films. Distinguishing frictional control from conformational gating, Journal of the American Chemical Society 125 (2003) 7704–7714.
[19] D.E. Khoshtariya, M. Shushanyan, R. Sujashvili, T.D. Dolidze, Dynamic and stochastic patterns of enzyme action. A key to the interpretation of "normal" and "small" solvent kinetic isotope effects (k^H/k^D), Journal of Biological Physics and Chemistry (Basel) 5 (2005) 103–110.
[20] D.E. Khoshtariya, T.D. Dolidze, M. Shushanyan, K.L. Davis, D.H. Waldeck, R. van Eldik, Fundamental signatures of short- and long-range electron transfer for azurin functionalized at Au/alkanethiol SAM junctions, Proceedings of the National Academy of Sciences of the United States of America 107 (2010) 2757–2762.
[21] P.L. Privalov, N.N. Khechinashvili, A thermodynamic approach to the problem of stabilization of globular protein structure: a calorimetric study, Journal of Molecular Biology 86 (1974) 665–684.
[22] N.N. Khechinashvili, J. Janin, F. Rodier, Thermodynamics of the temperature-induced unfolding of globular proteins, Protein Science 4 (1995) 1315–1324.
[23] E. Freire, W.W. van Osdol, O.L. Mayorga, J.M. Sanches-Ruiz, Calorimetricaly determined dynamics of complex unfolding transitions in proteins, Annual Review of Biophysics and Biophysical Chemistry 19 (1990) 159–188.
[24] J.M. Sanches-Ruiz, Theoretical analysis of Lumry–Eyring models in differential scanning calorimetry, Biophysical Journal 61 (1992) 921–935.
[25] C. La Rosa, D. Milardi, D. Grasso, R. Guzzi, L. Sporteli, Thermodynamics of the thermal unfolding of azurin, The Journal of Physical Chemistry 99 (1995) 14864–14870.
[26] H. Weingärtner, C. Cabrele, C. Herrmann, How ionic liquids can help to stabilize native proteins, Physical Chemistry Chemical Physics (2012), http://dx.doi.org/10.1039/c1cp21947b.
[27] M. Arai, K. Kuwajima, Role of the molten globule state in protein folding, Advances in Protein Chemistry 53 (2000) 209–282.
[28] P.L. Privalov, S.A. Potekhin, Scanning microcalorimetry in studying temperature-induced changes in proteins, Methods in Enzymology 131 (1986) 4–51.
[29] D. Martin, A. Weise, H.-J. Niclas, The solvent dimethyl sulfoxide, Angewandte Chemie, International Edition 6 (1967) 318–334.
[30] Z.-W. Yu, P.J. Quinn, Dimethyl sulphoxide: a review of applications in cell biology, Bioscience Reports 14 (1994) 259–281.
[31] K. Capriotti, J.A. Capriotti, Dimethyl sulfoxide: history, chemistry, and clinical utility in dermatology, The Journal of Clinical and Aesthetic Dermatology 5 (2012) 24–26.
[32] A.N. Rajeshwara, V. Prakash, Structural stability of lipase from wheat germ, International Journal of Peptide and Protein Research 44 (1994) 435–440.
[33] S. Rajendran, C. Radha, V. Prakash, Mechanism of solvent-induced thermal stabilization of alfa-amylase from *Bacillus amyloliquefaciens*, International Journal of Peptide and Protein Research 45 (1995) 122–128.
[34] K. Hamaguchi, Structure of muramidase (lysosyme). VIII. Effect of dimethyl sulfoxide on the stability of muramidase, Journal of Biochemistry (Tokyo) 56 (1964) 441–449.
[35] M. Kotik, S.E. Radford, C.M. Dobson, Comparison of the refolding of hen lysozyme from dimethyl sulfoxide and guanidinium chloride, Biochemistry 34 (1995) 1714–1724.
[36] I.K. Voets, W.A. Cruz, C. Moitzi, P. Lindner, E.P.G. Areas, P. Schurtenberger, DMSO-induced denaturation of hen egg white lysozyme, The Journal of Physical Chemistry. B 114 (2010) 11875–11883.
[37] R.L. Perlman, J. Wolff, Dimethyl sulfoxide: an inhibitor of liver alcohol dehydrogenase, Science (Washington) 160 (1968) 317–319.
[38] M. Banasik, K. Ueda, Dual inhibitory effects of dimethyl sulfoxide on poly(adp-ribose) synthetase, Journal of Enzyme Inhibition 14 (1999) 239–250.
[39] O. Almarsson, A.M. Klibanov, Remarkable activation of enzymes in nonaqueous aqueous media by denaturing organic cosolvents, Biotechnology and Bioengineering (1996) 4987–4992.
[40] H.J. Zhang, X.R. Sheng, X.M. Pan, J.M. Zhou, Activation of adenylate kinase by denaturants is due to the increasing conformational flexibility at its active sites, Biochemical and Biophysical Research Communications 113 (1983) 348–352.
[41] A. Steinschneider, K. Druck, Ribonuclease properties and activity in the presence of dimethylsulfoxide, Biochimica et Biophysica Acta 287 (1972) 77–89.
[42] J.E. Lovelock, M.W.H. Bishop, Prevention of freezing damage to living cells by dimethyl sulphoxide, Nature (London) 183 (1959) 1394–1395.
[43] E. Jaspard, Role of protein–solvent interactions in refolding: effects of cosolvent additives on the renaturation of porcine pancreatic elastase at various pHs, Archives of Biochemistry and Biophysics 375 (2000) 220–228.
[44] W.-B. Ou, Y.-D. Park, H.-M. Zhou, Effect of osmolytes as folding aids on creatine kinase refolding pathway, The International Journal of Biochemistry & Cell Biology 34 (2002) 136–147.
[45] S.-H. Kim, Y.-B. Yan, H.-M. Zhou, Role of osmolytes as chemical chaperones during the refolding of aminoacylase, Biochemistry and Cell Biology 84 (2006) 30–38.
[46] B. Zerner, M.L. Bender, The kinetic consequences of the acyl-enzyme mechanism for the reactions of specific substrates with chymotrypsin, Journal of the American Chemical Society 86 (1964) 3669–3674.
[47] N.L. Eremeev, Interaction of α-chymotrypsin with dimethyl sulfoxide: a change of substrate could "change" the interaction mechanism, Bioorganicheskaia Khimiia 29 (2003) 479–485.
[48] C.L. Tsou, Conformational flexibility of enzyme active sites, Science 262 (1993) 380–381.
[49] C.L. Tsou, Active site flexibility in enzyme catalysis, Annals of the New York Academy of Sciences 864 (1998) 1–8.
[50] J. Bhalla, G.B. Storchan, C.M. MacCarthy, V.N. Uversky, O. Tcherkasskaya, Local flexibility in molecular function paradigm, Molecular & Cellular Proteomics 5 (2006) 1212–1223.
[51] D.E. Khoshtariya, V.V. Topolev, L.I. Krishtalik, Study of proton transfer in enzymatic hydrolysis by the method of temperature dependence of kinetic isotope effect. I.

α-chymotrypsin catalyzed hydrolysis of N-acetyl- and N-benzyl-L-tyrosine ethyl esters, Bioorganicheskaia Khimiia 4 (1978) 1341–1351.
[52] D.E. Khoshtariya, Study of proton transfer in enzymatic hydrolysis by the method of temperature dependence of kinetic isotope effect. II. β-trypsin catalyzed hydrolysis of N-benzoyl-L-arginine ethyl ester, Bioorganicheskaia Khimiia 4 (1978) 1673–1677.
[53] L.Z. Holland, M. McFall-Ngai, G.N. Somero, Evolution of lactate dehydrogenase-A homologs of barracuda fishes (*Genus Sphyraena*) from different thermal environments: differences in kinetic properties and thermal stability are due to amino acid substitutions outside the active site, Biochemistry 36 (1997) 3207–3215.
[54] P.A. Fields, G.N. Somero, Hot spots in cold adaptation: localized increases in conformational flexibility in lactate dehydrogenase A4 orthologs of Antarctic notothenioid fishes, Proceedings of the National Academy of Sciences of the United States of America 95 (1998) 11476–11481.
[55] F. Conejero-Lara, A.I. Azuaga, P.L. Mateo, Differential scanning calorimetry of thermolysin and its 255–316 and 205–316 C-terminal fragments, Reactive and Functional Polymers 34 (1997) 113–120.
[56] F. Conejero-Lara, V. De Filippis, A. Fontana, P.L. Mateo, The thermodynamics of the unfolding of an isolated protein subdomain: the 255–316 C-terminal fragment of thermolysin, FEBS Letters 344 (1994) 154–156.
[57] J. Wen, K. Arthur, L. Chemmalil, S. Muzammil, J. Gabrielson, Y. Jiang, Applications of differential scanning calorimetry for thermal stability analysis of proteins: qualification of DSC, Journal of Pharmaceutical Sciences 101 (2012) 955–964.
[58] D.E. Khoshtariya, M. Makharadze, G. Getashvili, M. Zaalishvili, On the DSC rate performance for a three-state thermal denaturation of globular proteins, Bulletin of the Georgian National Academy of Sciences 164 (2001) 535–537.
[59] D.E. Khoshtariya, N.G. Goguadze, Conformationally-adiabatic process of deacylation of N-acetyl-L-tyrosile-α-chymotrypsin, Bioorganicheskaia Khimiia 11 (1985) 1621–1626.
[60] D.E. Khoshtariya, N.G. Goguadze, J. Ulstrup, Kinetic manifestation of conformational dynamics accompanying enzymatic hydrolysis of benzoyl-glycyl-phenillactate by carcoxypeptidase A, Bioorganicheskaia Khimiia 17 (1991) 618–625.
[61] Y. Fujita, S. Izumiguchi, Y. Noda, Effect of dimethylsulfoxide and its homologues on the thermal denaturation of lysozyme as measured by differential scanning calorimetry, International Journal of Peptide and Protein Research 19 (1982) 25–31.
[62] A. Torreggiani, M.D. Foggia, L. Manco, A. De Maio, S.A. Markarian, S. Bonora, Effect of sulfoxides on the thermal denaturation of hen lysozyme: a calorimetric and Raman study, Journal of Molecular Structure 891 (2008) 115–122.
[63] T. Arakawa, Y. Kita, S.N. Timasheff, Protein precipitation and denaturation by dimethyl sulfoxide, Biophysical Chemistry 131 (2007) 62–70.
[64] Y. Fujita, A. Miyanaga, Y. Noda, Effect of alcohols on the thermal denaturation of lysozyme as measured by differential scanning calorimetry, Bulletin of the Chemical Society of Japan 52 (1979) 3659–3662.
[65] G. Velicelebi, J.M. Sturtevant, Thermodynamics of the denaturation of lysozyme in alcohol–water mixtures, Biochemistry 18 (1979) 1180–1186.
[66] P. Attri, P. Venkatesu, M.J. Lee, Influence of osmolytes and denaturants on the structure and enzyme activity of alpha-chymotrypsin, The Journal of Physical Chemistry. B 114 (2010) 1471–1478.
[67] A. Kumar, P. Attri, P. Venkatesu, Effect of polyols on the native structure of alpha-chymotrypsin: a comparable study, Thermochimica Acta 536 (2012) 55–62.
[68] H. Jóhannesson, V.P. Denisov, B. Halle, Dimethyl sulfoxide binding to globular proteins: a nuclear magnetic relaxation dispersion study, Protein Science 6 (1997) 1756–1763.
[69] S. Bhattacharjya, P. Balaram, Effects of organic solvents on protein structures: observation of a structured helical core in hen egg-white lysozyme in aqueous dimethylsulfoxide, Proteins 29 (1997) 492–507.
[70] A. Giugliarelli, M. Paolantoni, A. Morresi, P. Sassi, Denaturation and preservation of globular proteins: the role of DMSO, The Journal of Physical Chemistry. B 116 (2012) 13361–13367.
[71] Y.J. Zhen, R.L. Ornstein, A molecular dynamics and quantum mechanics analysis of the effect of DMSO on enzyme structure and dynamics: subtilisin, Journal of the American Chemical Society 118 (1996) 4175–4180.
[72] S. Roy, B. Jana, B. Bagchi, Dimethyl sulfoxide induced structural transformations and non-monotonic concentration dependence of conformational fluctuation around active site of lysozyme, The Journal of Chemical Physics 136 (115103) (2012) 1–10.
[73] D.M. Segal, J.C. Powers, G.H. Cohen, D.R. Davies, P.E. Wilcox, Substrate binding site in bovine chymotrypsin A_γ. Crystallographic study using peptide chloromethyl ketones as site-specific inhibitors, Biochemistry 10 (1971) 3728–3739.
[74] J.C. Powers, B.L. Baker, J. Browb, B.K. Chelm, Inhibition of chymotrypsin A-alpha with N-acyl- and N-peptidyl-2-phenylethylamines. Subsite binding free energies, Journal of the American Chemical Society 96 (1974) 238–243.
[75] D.M. Segal, Kinetic investigation of the crystallographically deduced binding subsites of bovine chymotrypsin Aγ, Biochemistry 11 (1972) 349–356.
[76] S.A. Bizzozero, W.K. Baumann, H. Dutler, Kinetic investigation of the α-chymotrypsin-catalyzed hydrolysis of peptide-ester substrates, European Journal of Biochemistry 58 (1975) 167–176.
[77] C.-A. Bauer, The active centers of *Streptomyces griseus* protease 3 and α-chymotrypsin: enzyme–substrate interactions beyond subsite S_1', Biochimica et Biophysica Acta 438 (1976) 495–502.
[78] S.N. Timasheff, G. Xie, Preferential interactions of urea with lysozyme and their linkage to protein denaturation, Biophysical Chemistry 105 (2003) 421–448.
[79] B.J. Bennion, V. Daggett, Counteraction of urea-induced protein denaturation by trimethylamine N-oxide: a chemical chaperone at atomic resolution, Proceedings of the National Academy of Sciences of the United States of America 101 (2004) 6433–6438.
[80] A. Kumar, P. Venkatesu, Overview of the stability of α-chymotrypsin in different solvent media, Chemical Reviews 112 (2012) 4283–4307.
[81] P.J. Rossky, Protein denaturation by urea: slash and bond, Proceedings of the National Academy of Sciences of the United States of America 105 (2008) 16825–16826.
[82] L. Hua, R. Zhou, D. Thirumalai, B.J. Berne, Urea denaturation by stronger dispersion interactions with proteins than water implies a two-stage unfolding, Proceedings of the National Academy of Sciences of the United States of America 105 (2008) 16928–16933.
[83] S.C. Mande, M.E. Sobhia, Structural characterization of protein–denaturant interactions: crystal structures of hen egg-white lysozyme in complex with DMSO and guanidinium chloride, Protein Engineering 13 (2000) 133–141.
[84] P.H. Yancey, G.N. Somero, Methylamine osmoregulatory solutes of elasmobranch fishes counteract urea inhibition of enzymes, The Journal of Experimental Zoology 212 (1980) 205–213.
[85] H. Frauenfelder, G.A. Petsko, D. Tsernoglou, Temperature-dependent X-ray diffraction as a probe of protein structural dynamics, Nature (London) 280 (1979) 558–563.
[86] P.J. Artymiuk, C.C.F. Blake, D.E.P. Grace, S.J. Oatley, D.C. Phillips, M.J.E. Sternberg, Crystallographic studies of the dynamic properties of lysozyme, Nature (London) 280 (1979) 563–568.
[87] E.R. Birnbaum, F. Abbott, J.E. Gomez, D.W. Darnall, The calcium ion binding site in bovine chymotrypsin A, Archives of Biochemistry and Biophysics 179 (1977) 469–476.
[88] F. Adebodun, F. Jordan, Multinuclear magnetic resonance studies on the calcium(II) binding site in trypsin, chymotrypsin, and subtilisin, Biochemistry 28 (1989) 7524–7531.
[89] E. Fioretti, M. Angeletti, G. Lupidi, M. Coletta, Heterotropic modulation of the protease–inhibitor-recognition process: cations effect the binding properties of α-chymotrypsin, European Journal of Biochemistry 225 (1994) 459–465.
[90] K. Kar, B. Alex, N. Kishore, Thermodynamics of the interactions of calcium chloride with α-chymotrypsin, The Journal of Chemical Thermodynamics 34 (2002) 319–336.
[91] J.J. Birktoft, D.M. Blow, Structure of crystalline α-chymotrypsin. V. the atomic structure of tosyl-α-chymotrypsin at 2 Å resolution, Journal of Molecular Biology 68 (1972) 187–240.
[92] C.N. Pace, Conformational stability of globular proteins, Trends in Biochemical Sciences 15 (1990) 14–17.
[93] N. Ui, Isoelectric points and conformation of proteins. II Isoelectric focusing of α-chymotrypsin and its inactive derivative, Biochimica et Biophysica Acta 229 (1971) 582–589.
[94] S.N. Timasheff, The control of protein stability and association by weak interactions with water. How do solvent affect these processes? Annual Review of Biophysics and Biomolecular Structure 22 (1993) 67–97.
[95] C.N. Pace, D.V. Laurence, J.A. Thomson, pH dependence of the urea and guanidine hydrochloride denaturation of ribonuclease A and ribonuclease T1, Biochemistry 29 (1990) 2564–2572.
[96] A.-S. Yang, B. Honig, On the pH dependence of protein stability, Journal of Molecular Biology 231 (1993) 459–474.
[97] A.H. Elcock, Realistic modelling of the denatured states of proteins allows accurate calculations of the pH dependence of protein stability, Journal of Molecular Biology 294 (1999) 1051–1062.
[98] G.I. Makhatadze, P.L. Privalov, Contribution of hydration to protein folding thermodynamics. I. The enthalpy of hydration, Journal of Molecular Biology 232 (1993) 639–659.
[99] G.I. Makhatadze, P.L. Privalov, Energetics of protein structure, Advances in Protein Chemistry 47 (1995) 307–425.
[100] S.S. Stickler, A.V. Gribenko, A.V. Gribenko, T.R. Keiffer, J. Tomilson, T. Reihle, V.V. Loladze, G.I. Makhatadze, Protein stability and surface electrostatics: a charged relationship, Biochemistry 45 (2006) 2761–2766.
[101] A.G. Gvritishvili, A.V. Gribenko, G.I. Makhatadze, Cooperativity of complex salt bridges, Protein Science 17 (2008) 1285–1290.
[102] V.M. Dadarlat, C.B. Post, Contribution of charged groups to the enthalpic stabilization of the folded states of globular proteins, The Journal of Physical Chemistry. B 112 (2008) 6159–6167.
[103] L. Xiao, B. Honig, Electrostatic contributions to the stability of hyperthermophilic proteins, Journal of Molecular Biology 289 (1999) 1435–1444.
[104] G.R. Grimsley, K.I. Shaw, L.R. Fee, R.W. Alston, B.M.P. Huyghes-Despointes, R.L. Thurlkill, J.M. Scholtz, C.N. Pace, Increasing protein stability by altering long-range coulombic interactions, Protein Science 8 (1999) 1843–1849.
[105] G. Careri, Cooperative charge fluctuations by migrating protons in globular proteins, Progress in Biophysics and Molecular Biology 70 (1998) 223–249.
[106] D.E. Khoshtariya, E. Hansen, R. Leecharoen, G.C. Walker, Probing protein hydration by the difference HO-H (HO-D) vibrational spectroscopy: interfacial percolation network involving highly polarizable water-water hydrogen bonds, Journal of Molecular Liquids 105 (2003) 13–36.
[107] B. Bagchi, Water dynamics in the hydration layer around proteins and micelles, Chemical Reviews 105 (2005) 3197–3219.
[108] V.A. Sirotkin, A.V. Khadiulina, Hydration of α-chymotrypsin: excess partial enthalpies of water and enzyme, Thermochimica Acta 522 (2011) 205–210.
[109] A. Wada, H. Nakamura, Nature of the charge distribution in proteins, Nature (London) 293 (1981) 757–758.
[110] D.E. Khoshtariya, T.D. Dolidze, P. Lindqvist-Reis, A. Neubrand, R. van Eldik, Liquid water (D_2O): a dynamic model emerging from near-infrared DO-D stretching overtone studies, Journal of Molecular Liquids 96 (97) (2002) 45–63.
[111] D.E. Khoshtariya, A. Zahl, T.D. Dolidze, A. Neubrand, R. van Eldik, Discrimination of diverse (pressure/temperature-dependent/independent) inherent sub-structures in liquid water (D_2O) from difference vibrational spectroscopy, The Journal of Physical Chemistry. B 108 (2004) 14796–14799.

[112] N.N. Khechinashvili, S.A. Volchkov, A.V. Kabanov, G. Barone, Thermal stability of proteins does not correlate with the energy of intramolecular interactions, Biochimica et Biophysica Acta 1784 (2008) 1830–1834.
[113] J.L. England, G. Haran, Role of solvation effects in protein denaturation: from thermodynamics to single molecules and back, Annual Review of Physical Chemistry 62 (2011) 257–277.
[114] J. Bush, G.I. Makhatadze, Statistical analysis of protein structures suggests that buried ionisable residues in proteins are hydrogen bonded or form salt bridges, Proteins 79 (2011) 2027–2032.
[115] M. Ohgushi, A. Wada, Molten-globule state: a compact form of globular proteins with mobile side chains, FEBS Letters 164 (1983) 21–24.
[116] O.B. Ptytsin, The molten globule state, in: T.E. Creighton (Ed.), Protein Folding, Freeman, New York, 1992, pp. 243–300.
[117] Y.V. Griko, P.L. Privalov, Thermodynamic puzzle of apomyoglobin unfolding, Journal of Molecular Biology 235 (1994) 1318–1325.
[118] Y.V. Griko, Energetic basis of structural stability in the molten globule state: α-lactalbumin, Journal of Molecular Biology 297 (2000) 1259–1268.